Reversible Storage of Molecular Hydrogen by Sorption into Multilayered TiO_2 Nanotubes

Dmitry V. Bavykin,*,† Alexei A. Lapkin,† Pawel K. Plucinski,† Jens M. Friedrich,‡ and Frank C. Walsh‡

Catalysis and Reaction Engineering Group, Department of Chemical Engineering, University of Bath, Bath, BA2 7AY, United Kingdom, and Electrochemical Engineering Group, School of Engineering Sciences, University of Southampton, Highfield, Southampton SO17 1BJ, United Kingdom

Received: July 4, 2005; In Final Form: August 17, 2005

The sorption of hydrogen between the layers of the multilayered wall of nanotubular TiO_2 was studied in the temperature range of −195 to 200 °C and at pressures of 0 to 6 bar. Hydrogen can intercalate between layers in the walls of TiO_2 nanotubes forming host−guest compounds $TiO_2 \cdot xH_2$, where $x \leq 1.5$ and decreases at higher temperatures. The rate of hydrogen incorporation increases with temperature and the characteristic time for hydrogen sorption in TiO_2 nanotubes is several hours at 100 °C. The rate of intercalate formation is limited by the diffusion of molecular hydrogen inside the multilayered walls of the TiO_2 nanotube. ^{1}H NMR-MAS and XRD data confirm the incorporation of hydrogen between the layers in the walls of TiO_2 nanotubes. The nature and possible applications of the observed intercalates are considered.

Introduction

Environmental and supply problems related to the use of fossil fuels have stimulated the search for alternative sources of energy. Hydrogen is a favored candidate, having a high calorific value and producing only water on oxidation. However, the successful implementation of the hydrogen economy into industry raises the challenges of storage and transportation of hydrogen.[1] Recent approaches to hydrogen storage have considered adsorption of hydrogen on solids of large surface area, hydrogen storage by metal hydrides, and intercalation of molecular hydrogen in clathrate hydrates. A number of materials with nanotubular morphology have been studied as hydrogen adsorbents, including carbon,[2] boron nitride,[3] MoS_2,[4] and TiS_2.[5] Carbon nanotubes are the most intensively studied adsorbents for hydrogen, where dissociative chemisorption of hydrogen is catalyzed by various metals or by graphite edge sites, since it is possible to achieve a relatively high uptake of hydrogen under ambient conditions.[6,7] The use of metal hydrides allows a higher hydrogen uptake but requires higher temperatures for desorption of hydrogen and recycling of metal.[8]

The recent discovery[9] of hydrogen clathrate hydrate, $(32 + x)H_2 \cdot 136H_2O$, opens up the possibility of incorporating molecular hydrogen into the cage of water molecules such that dissociation of hydrogen can be avoided and high uptake of hydrogen can be achieved. In such a clathrate hydrate, the molecule of hydrogen is stabilized by several OH groups through hydrogen bonding.[10,11] It is necessary, however, to apply an extremely high pressure of hydrogen to promote self-organization of water and introduction of hydrogen molecules into the clathrate structure. A breakthrough can be anticipated by the use of preformed "host" structure to accommodate hydrogen "guest" molecules. Such host structures should have several OH groups and cavities of suitable geometry, where the pore diameter is larger than the dynamic diameter of a free hydrogen molecule ($d_1 = 0.4059$ nm[8]). A possible candidate for such "host" structures is provided by recently synthesized multilayered TiO_2 nanotubes[12] which have multilayered walls. The interstitial spacings between layers ($d_2 = 0.72$ nm) contain ion-exchangeable OH groups[13] which could accommodate hydrogen molecules.

This paper presents early observations of significant adsorption of molecular hydrogen into the pores of TiO_2 nanotubes. Systematic studies of the effect of pressure and temperature on the dynamics of hydrogen adsorption are presented. The nature of hydrogen incorporated into the structure of TiO_2 nanotubes and possible practical applications are discussed.

Experimental Details

Preparation and Characterization of TiO_2 Nanotubes. The method of preparation of TiO_2 nanotubes was based on alkali hydrothermal transformation.[14] Titanium dioxide (9 g) was added to 300 mL of 10 M NaOH solution and the mixture was heated for 22 h at 140 °C. The white, powdery TiO_2 was thoroughly washed with water then with 0.05 M H_2SO_4, followed by vacuum drying at 80 °C. HRTEM images were obtained with a JEM-100CX electron microscope with carbon sample grids. SEM images were obtained with a JEOL 6310 scanning electron microscope. XRD patterns were recorded on a Philips PW1710 diffractometer, with Cu Kα radiation $\lambda = 0.154$ nm and a graphite monochromator in the 2θ range of 10−80°. The BET area and BJH pore size distributions of the samples were measured, using nitrogen adsorption, on a Micromeritics ASAP 2010 instrument.

Hydrogen Adsorption Studies. Research grade purity hydrogen (99.999%) was used in all experiments. Adsorption of hydrogen was studied with use of an Intelligent Gravimetric Analyzer IGA-001 (Hiden Isochema, UK), having a sensitivity of 0.0001 mg. A TiO_2 nanotube sample (100 mg) was sealed in the reactor equipped with a temperature control unit. Measurements of the kinetics of hydrogen adsorption involved the following sequence: the sample was degassed at 200 °C for 2 h, the temperature was set to the desired value, the

* To whom correspondence should be addressed. Phone: +44-1225-384483. Fax: +44-1225-385713. E-mail: d.v.bavykin@bath.ac.uk.
† University of Bath.
‡ University of Southampton.

10.1021/jp0536394 CCC: $30.25
Published on Web 09/21/2005

hydrogen pressure was ramped from 0 bar to the set pressure with a ramp rate of 120 mbar min^{-1}, and the dynamics of sample weight change were followed. The stability of temperature was within 1 °C while the pressure stability was <0.5 mbar. The maximum fluctuation of hydrogen uptake after TiO_2 nanotubes saturation was 0.01 wt %. Adsorption isotherms were measured at −195 °C by using a standard sequence with a 30 min timeout for each point. During the hydrogen sorption experiments, the TiO_2 nanotubes were subjected to 10 adsorption/desorption cycles, and demonstrated a high level of reversibility.

^1H MAS NMR spectra with high-power proton decoupling were recorded at 400.13 MHz, on a Bruker MSL-400 spectrometer. Chemical shifts were adjusted to TMS with an accuracy of ±0.2 ppm via an external reference sample. During measurements, dried and sealed samples in glass ampules were opened then placed into the rotor and recorded at room temperature in an air atmosphere.

Results and Discussion

The titanium dioxide nanotubes produced by hydrothermal treatment of raw TiO_2 with 10 M NaOH typically have a tubular morphology with an internal diameter (d_t) in the range 2−10 nm and a tube length of 0.5 to 10 μm. The walls of the nanotubes consist of more then two layers and spacing between layers, $d_2 = 0.72$ nm (see Figure 1a,b). Each layer consists of a TiO_6 edge sharing octahedron building up a zigzag structure having $d_3 = 0.33$ nm for each step. During the folding of these layers to nanotubes, the chirality number is not equal to zero, resulting in an angle (α not equal to 90°) between the wall plane and chain of TiO_6 octahedrons (see Figure 1a). The exact crystal structure of TiO_2 nanotubes is currently disputed, proposals including $H_2Ti_3O_7$,[15] $H_2Ti_2O_4(OH)_2$,[16] or $H_2Ti_4O_9 \cdot H_2O$.[17] In all of these structures, OH groups or O atoms in the topmost corner positions (as well as in edge sharing positions) occupy positions on two sides of the nanotube surface (convex and concave) as well as in the interstitial cavities between the layers in the nanotube wall. Almost all protons of these OH groups can be easily exchanged with alkali metal cations[16,18] or with transition metal cations,[19] in aqueous solution. Some of the bulky cations can intercalate into the interstitial cavities between the layers in TiO_2 nanotube walls.[20] The interstitial cavities, however, were found to be inaccessible to nitrogen molecules.[14] The TiO_2 nanotubular, mesoporous materials studied here have a BET surface area equal to 199 $m^2\ g^{-1}$ (energy constant $c = 63$), an average BJH pore size of 8 nm, and a BJH pore volume of 0.70 $cm^3\ g^{-1}$.

The hydrogen adsorption isotherm for the TiO_2 nanotubes at −195 °C is shown in Figure 2. The hydrogen uptake is relatively high; almost 1.5 hydrogen molecules per one Ti atom can be adsorbed at a 2 bar pressure of hydrogen. Further increase in the hydrogen pressure does not significantly change the hydrogen uptake. During the desorption of hydrogen, a large hysteresis is observed; even at 0 bar of pressure, the uptake of hydrogen achieves a 1.25 molar ratio (point B in Figure 2). Remarkably, heating the sample in a vacuum to 200 °C leads to a complete desorption of hydrogen, returning the weight of the sample to its initial value (point A in Figure 2). Such behavior indicates that adsorption of hydrogen is a reversible process that occurs without formation of stable hydrides (this would lead to point B being above point A) and in the absence of redox processes followed by the elimination of lattice oxygen (this would lead to point B being below point A). Physical adsorption of hydrogen on TiO_2 nanotubes alone could not provide such a high value of observed hydrogen uptake. Taking

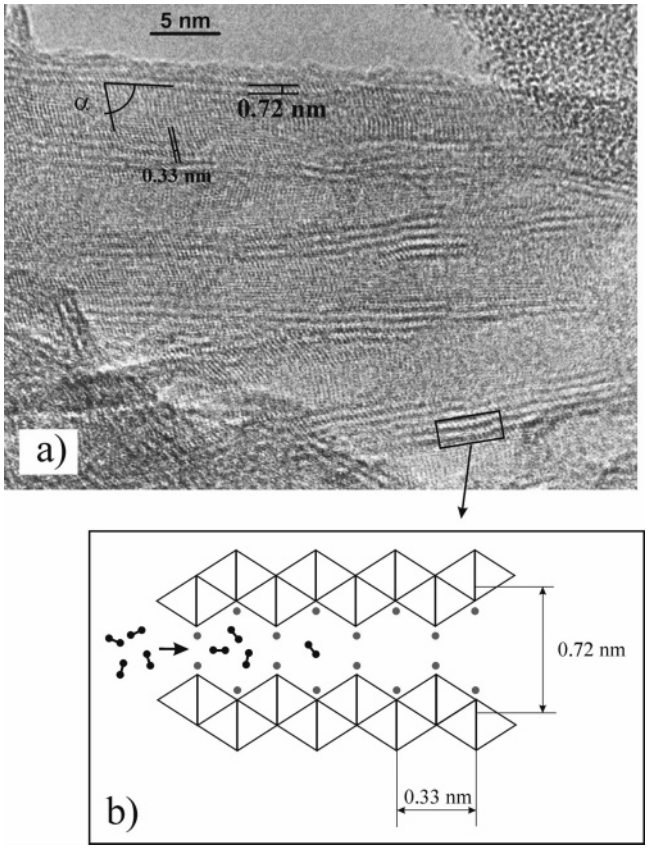

Figure 1. (a) HRTEM image of TiO_2 nanotubes showing nonzero chirality ($\alpha \neq 90°$), interlayer distance, and lattice parameter; (b) a cartoon of the proposed structure[15] for $H_2Ti_3O_7$, consisting of two layers separated by an interstitial cavity; molecular hydrogen can be incorporated in the cavity; ●, protons in $H_2Ti_3O_7$ lattice, ●−●, molecular hydrogen.

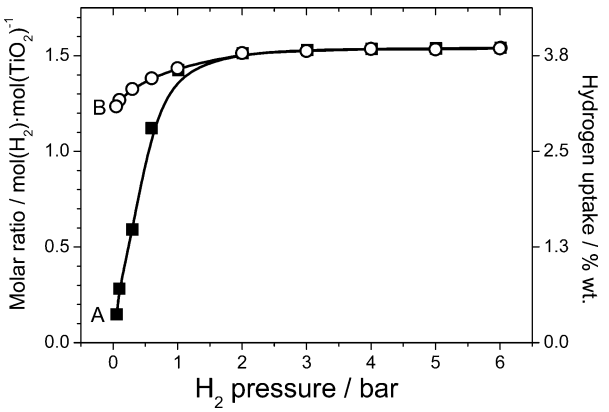

Figure 2. Isotherm for (■) hydrogen sorption into and (○) desorption out of the pores of TiO_2 nanotubes at −196 °C. The left axis represents the amount of hydrogen per unit amount of TiO_2.

the value of monolayer hydrogen density[8] as 1.3×10^{-5} mol m^{-2}, the maximum value of hydrogen adsorption on the surface of TiO_2 nanotubes can be calculated as 0.21 mol of hydrogen per mol of TiO_2. The observed value of adsorption is considerably higher, suggesting that hydrogen can occupy interstitial cavities between layers in the wall of nanotubes without chemical bond formation. Indeed, the size of interstitial cavities−zigzag slit pores ($d_2 = 0.72$ nm; see Figure 1b) is larger than the dynamic diameter of hydrogen molecules ($d_1 = 0.41$ nm) and much larger than the nuclear distance of hydrogen molecule ($d_0 = 0.07$ nm). OH groups in the nanotube lattice could stabilize the hydrogen molecules via weak van der Waals

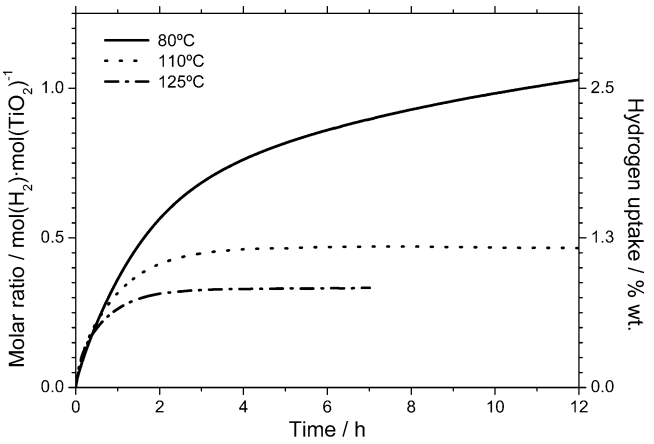

Figure 3. Kinetic curves for hydrogen intercalation into the TiO_2 nanotubes at temperatures in the range 80 to 125 °C and at a pressure of 1 bar. Before each experiment the sample was degassed at 200 °C for 2 h.

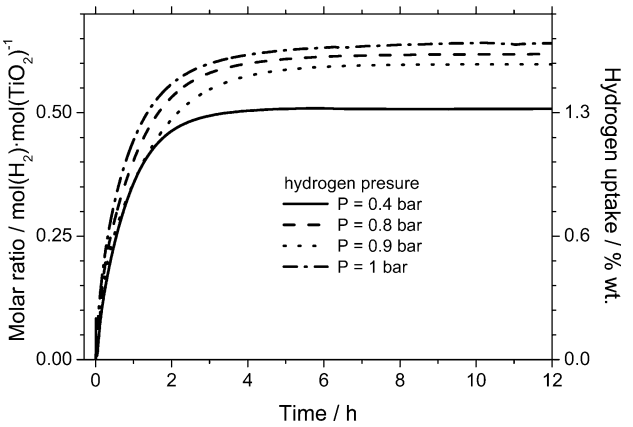

Figure 4. Kinetic curves for hydrogen intercalation into the TiO_2 nanotubes at pressures of hydrogen in the range 0.4 to 1 bar and at a temperature of 100 °C. Before each experiment the sample was degassed at 200 °C for 2 h.

interactions, resulting in formation of $TiO_2 \cdot xH_2$ clathrates (cf. the hydrogen clathrate hydrate $(32 + x)H_2 \cdot 136H_2O$[10]).

In contrast to ref 21 (which considers <2 wt % hydrogen uptake at a pressure of ~60 bar and room temperature), we have achieved a similar hydrogen sorption at 1 bar and temperatures in the range 80 to 125 °C. No kinetic data of sorption were provided in this reference; as shown below, such information can affect the interpretation of experimental hydrogen sorption and desorption data.

To understand the mechanism of intercalation of hydrogen into TiO_2 nanotubes, the kinetics of hydrogen adsorption into the cavities of TiO_2 nanotubes were studied. In Figure 3, the kinetic curves of intercalation of hydrogen into TiO_2 nanotubes at various temperatures are presented. It takes a relatively long time to achieve saturation of TiO_2 nanotubes with hydrogen (ca. 2 h at 110 °C and more than 10 h for temperatures below 80 °C). An increase in temperature results in a higher rate of achieving the steady-state uptake, demonstrating the activation controlled nature of hydrogen intercalation. On the other hand, an increase in temperature from 80 to 125 °C results in a lower steady-state molar ratio, down from almost 1 to less than 0.5, indicating that the process of intercalation is exothermic.

The fact that the characteristic time of hydrogen sorption (several hours) is much longer than the characteristic time of diffusion of hydrogen in the gas phase through the grains of powdered TiO_2 nanotubes or the time for setting the hydrogen pressure and temperature allow us to use the global hydrogen uptake for studying the kinetics of hydrogen sorption.

The effect of hydrogen pressure on the kinetics of hydrogen intercalation, measured at 100 °C, is shown in Figure 4. A decrease in hydrogen pressure from 1 to 0.4 bar resulted in a small decrease in the steady-state uptake of hydrogen from 0.6 to 0.5. A small inconsistency between sorption at 0.8 and 0.9 bar can be attributed to the difference in the history of the sample. It was also found that the rate of hydrogen intercalation into the TiO_2 nanotubes did not depend on the hydrogen pressure in the same range of hydrogen pressures. This phenomenon could be explained by the assumption that formation of hydrogen clathrate follows two consecutive steps:

$$H_{2,gas} \rightarrow H_{2,ads} \quad (1a)$$

$$H_{2,ads} \rightarrow H_{2,intercalate} \quad (1b)$$

where the first process of physical adsorption on the surface of TiO_2 nanotubes has a relatively short characteristic time, even for small pores, and the second process of transport of molecular hydrogen inside the interstitial cavities in the walls of TiO_2 nanotubes is the slow, rate-limiting step. The overall rate of hydrogen intercalation is then determined by the rate of hydrogen diffusion between the layers of multilayered walls in the TiO_2 nanotubes (see Figure 1b), which does not depend on the pressure of hydrogen in the gas phase.

The mechanism of diffusion of molecular hydrogen in solid materials has been intensively studied[22−24] and can be described via a hopping mechanism[25] where a hydrogen molecule hops from one cage to an adjacent one. It is possible to assume that transport of hydrogen in nanotubes occurs mainly along their length and that diffusion of hydrogen in the radial direction can be neglected. This assumption is supported by two facts. First, it was found[26] that the rate of hydrogen adsorption in nanotubular carbon could be improved by shortening the length of the tubes after sample milling. Second, the crystal structure of single layers in the multilayered nanotube wall consists of densely packed TiO_6 octahedrons (see Figure 1b), which are less likely to be penetrable by hydrogen molecules than the slit channels along the tube. The diffusion of molecular hydrogen in rodlike particles of length (l), where transport of hydrogen occurs only along the length of rods without hopping of hydrogen in the perpendicular direction (1-dimensional case[27]) can be described via:

$$y(t) = y_0\left[1 - \sum_n \frac{8}{(2n+1)^2\pi^2} e^{-D_{H_2}(2n+1)^2\pi^2 t/l^2}\right] \quad (2)$$

where y is the ratio of the number of hydrogen molecules incorporated inside the whole rod-like particle at the time t to the total number of titanium atoms in the particle (molar ratio), y_0 is the molar ratio at time infinity (steady-state uptake), and D_{H_2} is a diffusion coefficient of hydrogen along the length of the rod.

As shown in Figure 5, experimental data provided a good fit to eq 2, especially for kinetic data at higher temperatures. The lower temperature data result in a poorer fit, probably because of the change in the mechanism of hydrogen transport inside the walls of TiO_2 nanotubes. The TiO_2 nanotubes produced by alkali hydrothermal treatment are characterized by a relatively wide distribution in the nanotube length. The distribution of nanotubes in length is responsible for the existence of long tails in the kinetic curves due to the intercalation into the long tubes, which are always present in the sample.

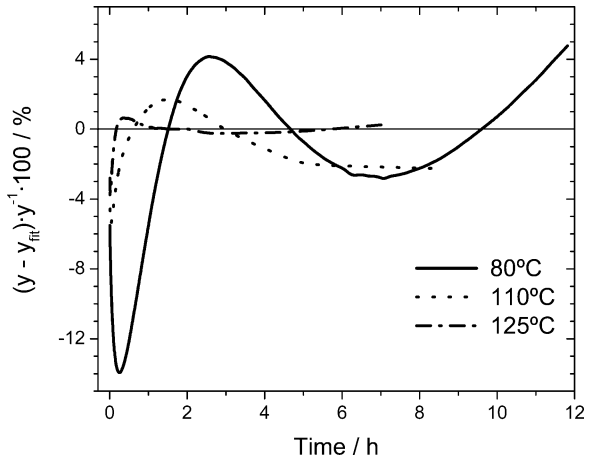

Figure 5. Deviation of experimental data (y) from the fitting curve (y_{fit}) derived from eq 2 for hydrogen intercalation into TiO_2 nanotubes at a pressure of 1 bar and at temperatures in the range 80 to 125 °C.

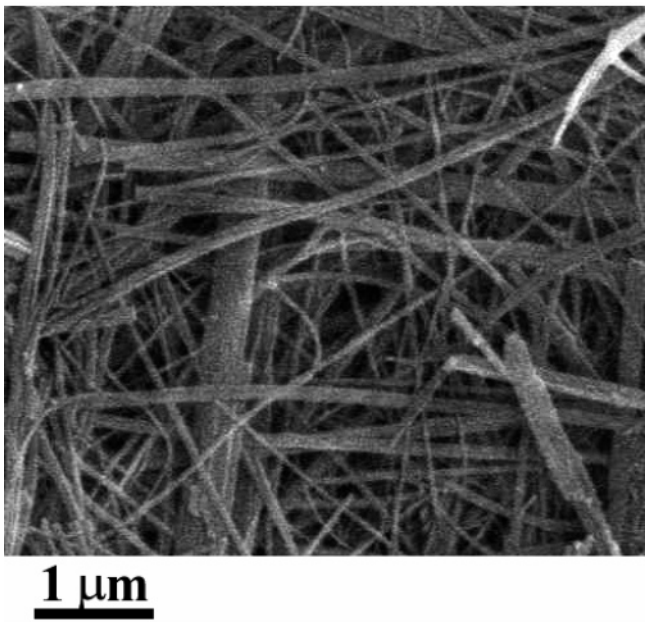

Figure 6. SEM image of long TiO_2 nanotubes.

The length of TiO_2 nanotubes produced during alkali hydrothermal treatment usually exceeds several microns (see Figure 6). For the fitting procedure, the following values of parameters in eq 2 have been used: $l = 4 \times 10^{-6}$ m, $n = 40$ (a further increase in n will not affect the results of calculations). The Runge−Kutta method of minimization of the square of deviations was used with y_0 and D_{H_2} as variables. The resulting values of diffusion coefficients and steady-state hydrogen uptake are summarized in Table 1. These observed values of diffusion coefficients are several orders of magnitude lower than typical values of diffusion coefficients of atomic hydrogen into the pores of solids,[28] supporting the hypothesis of a molecular form of the intercalating hydrogen. Analysis of the temperature dependence of the values of D_{H_2} and y_0 shows that the values of activation energy of diffusion of molecular hydrogen inside the walls of the TiO_2 nanotube and enthalpy of $TiO_2 \cdot xH_2$ clathrate formation in the range of temperatures from 80 °C to 125 °C are estimated at 44 and −30 kJ mol^{-1}, respectively. The value of diffusion activation energy is relatively high and may reflect the fact that oscillations of atoms in a crystal can modulate the width of the energy barrier between two cages, resulting in a strong dependence of diffusion coefficient on temperature.[29] The

TABLE 1: Results of Fitting Eq 2 to Experimental Kinetic Curves for Hydrogen Adsorption (Set Parameters Are $l = 4 \times 10^{-6}$ m and $n = 40$)

hydrogen pressure, bar	temp, °C	D_{H_2}, 10^{-12} cm^2 s^{-1}	y_0, $mol(H_2) \cdot mol(TiO_2)^{-1}$	standard deviation[a]
1	80	1.2	1.0	0.05
1	90	1.4	0.5	0.03
1	100	4.3	0.6	0.03
1	110	3.7	0.5	0.03
1	125	6.1	0.3	0.01
0.9	100	3.1	0.6	0.03
0.8	100	3.7	0.6	0.03
0.4	100	4.0	0.5	0.04

[a] Standard deviation was calculated by using the following formula: $(\sum_{i=0}^{m}(y_i - y_{i,fit})^2)^{1/2}/m - 1$, where m is the number of points used for fitting.

value of enthalpy of clathrate formation is also relatively high and probably includes interaction of hydrogen with the TiO_2 nanotube lattice.

The coefficient of self-diffusion of hydrogen for a hopping mechanism of diffusion could also be expressed by using the Einstein formula:

$$D_{H_2} = \frac{\lambda^2}{6\tau} \tag{3}$$

where λ is the short distance between two energy barriers (the hop length) and τ is the time interval between two hops. The value of λ could be equal to the distance between the two topmost corner O atoms from different TiO_6 octahedra in the chain, which is ca. 0.33 nm (see Figure 1b). The value of τ could be roughly estimated from the following NMR data.

The relatively slow desorption of hydrogen from the $TiO_2 \cdot xH_2$ clathrate at room temperature facilitates measurement of some physical and chemical properties of this intercalate. In Figure 7, the proton MAS NMR spectra of initial TiO_2 nanotube and nanotubes fully saturated with hydrogen $TiO_2 \cdot 1.5H_2$ measured at room temperature are shown. The spectrum of the initial dry sample of powdered TiO_2 nanotubes shows several relatively wide peaks having chemical shifts in the range 12 to 0 ppm. These are resonance signals from different protons of the TiO_2 nanotube lattice. The presence of water adsorbed into the pores of TiO_2 nanotubes results in the appearance of a massive signal at about 4 ppm[30] masking the fine structure of lattice protons. The signal of intercalated molecular hydrogen is also expected at 4.5 ppm[31] and it is very important to avoid any contact with water vapor during hydrogen sorption followed by ^1H MAS NMR study of TiO_2 nanotubes. The spectrum of molecular hydrogen intercalated into the TiO_2 nanotubes has a single narrow peak at 4.5 ppm. The width (fwhm) of the peak is equal to 1.2 ppm confirming the high mobility of intercalated hydrogen molecules. From this spectrum the order of value of the spin relaxation constant T_2 could be roughly estimated by using the following equation:

$$T_2 = \frac{1}{\pi(\mathrm{FWHM})} \tag{4}$$

and is approximately equal to 0.66 ms. If it is assumed that T_2 is equal to the time interval between two hops, τ, then using formula 3 we can estimate the coefficient of self-diffusion of hydrogen inside the walls of nanotubes at room temperature (25 °C) being ca. 2.8×10^{-13} cm^2 s^{-1}. This number is close to the value of 7.7×10^{-14} cm^2 s^{-1} produced by extrapolating

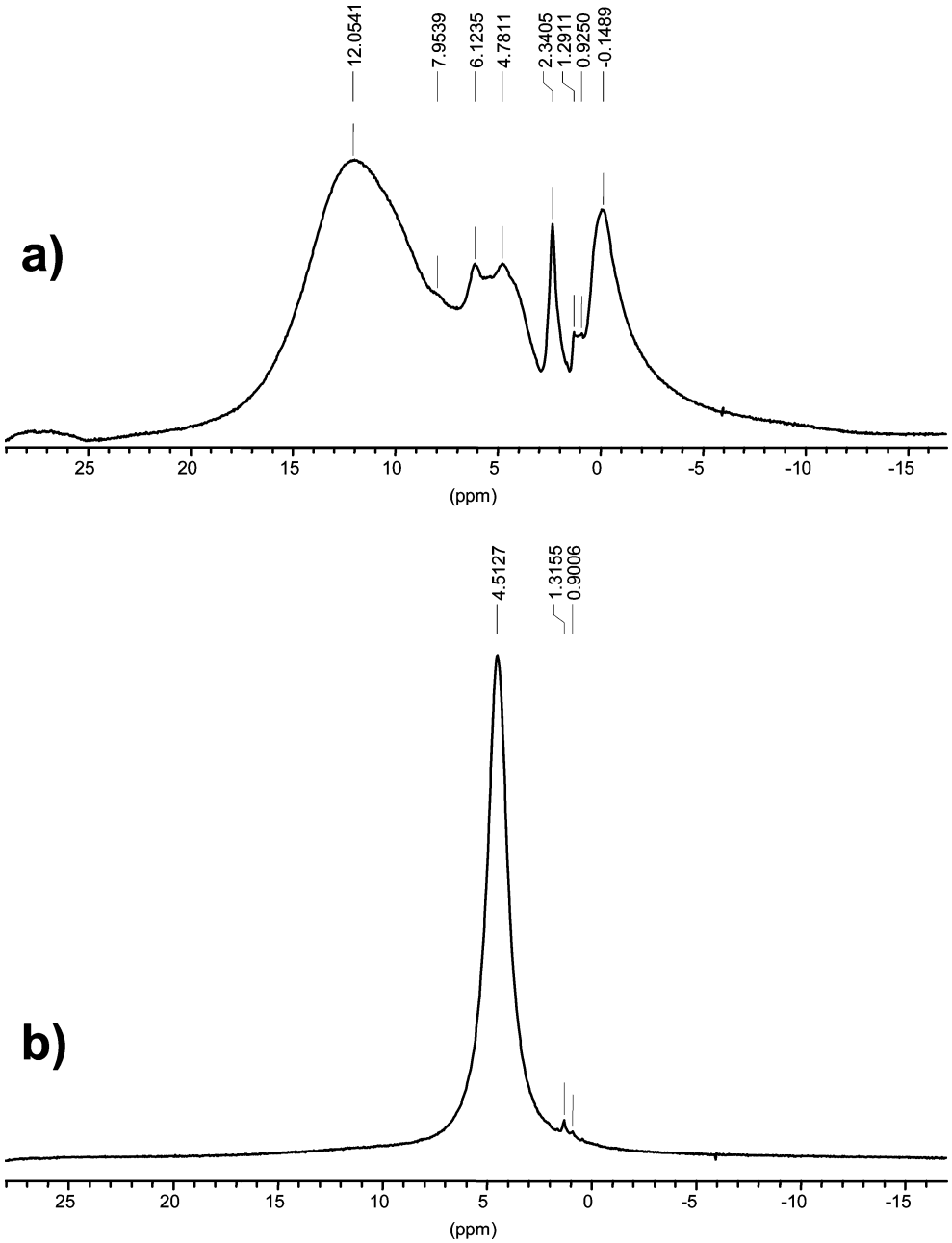

Figure 7. ^{1}H MAS NMR spectra at a temperature of 25 °C: (a) dry TiO_2 nanotubes and (b) molecular hydrogen intercalated into TiO_2 nanotubes. Signals at approximately 1.3 and 0.9 ppm are artifacts from the rotor.

toward lower temperatures the diffusion coefficient from direct kinetic measurements at higher temperatures, using formula 2 and the value of activation energy 44 kJ mol^{-1} for diffusion.

The intercalation of hydrogen inside the wall of nanotubes results in no significant change in crystal structure as demonstrated in Figure 8 where XRD patterns for both TiO_2 nanotubes and TiO_2 nanotubes saturated with hydrogen are shown. This reflects the earlier observed constancy of interlayer distance after intercalation of metal cations, which was attributed to the robustness of tubular morphology.[20] Sorption of hydrogen can also significantly change the electrical conductivity of tubular TiO_2[32,33] (>100 nm average diameter) produced by anodic oxidation. A similar behavior might be expected from TiO_2 nanotubes produced by alkali hydrothermal treatment, which have wide band gap, semiconductor optical properties.[34]

The combined properties of effective and reversible hydrogen sorption and simplicity of synthesis render TiO_2 nanotube materials possible candidates for development of hydrogen sensing and storage applications. In contrast to carbon nanotubes or metal alloy hydrides, TiO_2 nanotubes can also operate over a convenient range of pressures and temperatures. Moreover, simple pressure and temperature swings can be used to adsorb and desorb hydrogen from the solid state, nanotubular TiO_2.

It is possible that the rate of hydrogen sorption could be significantly improved by decreasing the length of TiO_2 nanotubes by using ultrasonic treatment[14] making the material more attractive for hydrogen storage and sensing applications.

Conclusions

1. The sorption of hydrogen to TiO_2 nanotube powders has been studied at temperatrures in the range of −195 to 200 °C and pressures of 0 to 6 bar with use of a precision gravimetric analyzer.

2. A relatively high and reversible hydrogen uptake has been demonstrated.

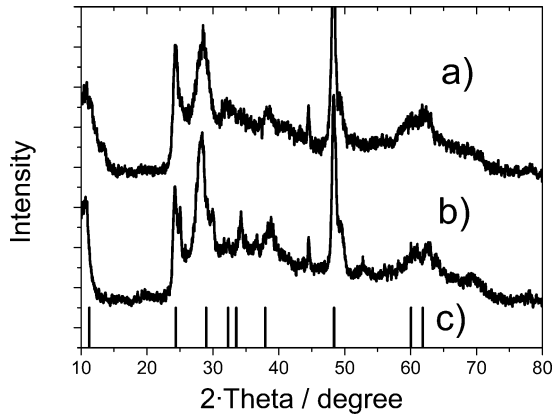

Figure 8. XRD patterns of (a) nanotubular TiO_2 saturated with sorbed hydrogen, (b) nanotubular TiO_2, as prepared, and (c) $H_2Ti_3O_7$ reflections according to Chen et al.[15]

3. The morphology of TiO_2 nanotubes and the mobility of incorporated hydrogen, revealed by ^1H MAS NMR, suggest that adsorption of hydrogen may occur in its molecular form with the formation of intercalate compounds $TiO_2 \cdot xH_2$.

4. Kinetic studies of molecular hydrogen intercalation support the hypothesis that diffusion of hydrogen molecules in the axial direction between the layers in multilayered walls of TiO_2 nanotubes is the rate-limiting step of the process of intercalation.

5. The effect of temperature on the regularities of clathrate formation has been studied and values of the diffusion activation energy of 44 kJ mol^{-1} and enthalpy of clathrate formation of -30 kJ mol^{-1} have been estimated.

6. From a proposed diffusion model, the rate of hydrogen intercalation depends on the reverse square of nanotube length.

Acknowledgment. The authors are grateful to Dr. A. G. Stepanov and Dr. E. P. Talzi (Boreskov Institute of Catalysis, Novosibirsk) for ^1H MAS NMR measurements and helpful discussion. This work was supported by EC project "CREATION" G5RD-CT-2002-00724.

References and Notes

(1) Dresselhaus, M. S.; Thomas, I. L. *Nature* **2001**, *414*, 332.

(2) Dillon, A. C.; Jones, K. M.; Bekkedahl, T. A.; Kiang, C. H.; Bethune, D. S.; Heben, M. J. *Nature* **1997**, *386*, 337.

(3) Ma, R.; Bando, Y.; Zhu, H.; Sato, T.; Xu, C.; Wu, D. *J. Am. Chem. Soc.* **2002**, *124*, 7672.

(4) Chen, J.; Li, S. L.; Tao, Z. L. *J. Alloys Comput.* **2003**, *356*−*357*, 413.

(5) Chen, J.; Li, S. L.; Tao, Z. L.; Shen, Y. T.; Cui, C. X. *J. Am. Chem. Soc.* **2003**, *125*, 5284.

(6) Browning, D. J.; Gerrard, M. L.; Lakeman, J. B.; Mellor, I. M.; Mortimer, R. J.; Turpin, M. C. *Nano Lett.* **2002**, Vol. 2, No. 3, 201.

(7) Kim, H. S.; Lee, H.; Han, K. S.; Kim, J. H.; Song, M. S.; Park, M. S.; Lee, J. Y.; Kang, J. K. *J. Phys. Chem. B* **2005**, *109*, 8983.

(8) Schlapbach, L.; Züttel, A. *Nature* **2001**, *414*, 353.

(9) Mao, W. L.; Mao, H. *Proc. Natl. Acad. Sci. U.S.A.* **2004**, *101*, 708.

(10) Lokshin, K. A.; Zhao, Y.; He, D.; Mao, W. L.; Mao, H. K.; Hemley, R. J.; Lobanov, M. V.; Greenblatt, M. *Phys. Rev. Lett.* **2004**, *93*, 125503.

(11) Suitte, B. P.; Belair, S. D.; Francisco, J. S. *Phys. Rev. A* **2004**, *70*, 033201.

(12) Kasuga, T.; Hiramatsu, M.; Hoson, A.; Sekino, T.; Niihara, K. *Adv. Mater.* **1999**, *11* (No. 15), 1307.

(13) Sun, X.; Li, Y. *Chem. Eur. J.* **2003**, *9*, 2229.

(14) Bavykin, D. V.; Parmon, V. N.; Lapkin, A. A.; Walsh, F. C. *J. Mater. Chem.* **2004**, *14*, 3370.

(15) Chen, Q.; Du, G. H.; Zhang Peng, S. L. M. *Acta Crystallogr. B* **2002**, *58*, 587.

(16) Yang, J. J.; Jin, Z. S.; Wang, X. D.; Li, W.; Zhang, J. W.; Zhang, S. L.; Guo, X. Y.; Zhang, Z. J. *Dalton Trans.* **2003**, *20*, 3898.

(17) Nakahira, A.; Kato, W.; Tamai, M.; Isshiki, T.; Nishio, K.; Aritani, H. *J. Mater. Sci.* **2004**, *39*, 4239.

(18) Armstrong, G.; Armstrong, A. R.; Canales, J.; Bruce, P. G. *Chem. Commun.* **2005**, 2454.

(19) Bavykin, D. V.; Lapkin, A. A.; Plucinski, P. K.; Friedrich, J. M.; Walsh, F. C. *J. Catal.* **2005**, *235*, 10.

(20) Ma, R.; Sasaki, T.; Bando Y. *Chem. Commun.* **2005**, *7*, 948.

(21) Lim, S. H.; Luo, J.; Zhong, Z.; Ji, W.; Lin, J. *Inorg. Chem.* **2005**, *44*, 4124.

(22) Kondratyev, V. V.; Gapontsev, A. V.; Voloshinskii, A. N.; Obukhov, A. G.; Timofeyev, N. I. *Int. J. Hydrogen Energy* **1999**, *24*, 819.

(23) Skoulidas, A. I.; Ackerman, D. M.; Johnson, J. K.; Sholl, D. S. *Phys. Rev. Lett.* **2002**, *89*, 185901.

(24) Harris, J. H.; Curting, W. A.; Tenhover, M. A. *Phys. Rev. B* **1987**, *36*, 5784.

(25) Van den Berg, A. W. C.; Bromley, S. T.; Flikkema, E.; Wojdel, J.; Maschmeyer, Th.; Jansen, J. C. *J. Chem. Phys.*, **2004**, *120*, 10285.

(26) Liu, F.; Zhang, X.; Cheng, J.; Tu, J.; Kong, F.; Huang, W.; Chen, C. *Carbon* **2003**, *41*, 2527.

(27) Crank, J. *The Mathematics of Diffusion*; Clarendon Press: Oxford, UK, 1956.

(28) Garberoglio, G.; Vallauri, R. *J. Mol. Liq.* **2005**, *117*, 43.

(29) Ilinitch, O. M.; Fenelonov, V. B.; Lapkin, A. A.; Okkel, L. G.; Terskikh, V. V.; Zamaraev, K. I. *Microporous Mesoporous Mater.* **1999**, *31*, 97.

(30) Thorne, A.; Kruth, A.; Tunstall, D.; Irvine, J. T. S.; Zhou, W. *J. Phys. Chem. B* **2005**, *109*, 5439.

(31) Lee, H.; Lee, J. W.; Kim, D. Y.; Park, J.; Seo, Y.-T.; Zeng, H.; Moudrakovski, I. L.; Ratcliffe, C. I.; Ripmeester, J. A. *Nature* **2005**, *434*, 743.

(32) Varghese, O. K.; Gong, D.; Paulose, M.; Ong, K. G.; Grimes, C. A. *Sens. Actuators, B* **2003**, *93*, 338.

(33) Mor, G. K.; Carvalho, M. A.; Varghese, O. K.; Pishko, M. V.; Grimes, C. A. *J. Mater. Res.* **2004**, *19*, 2, 628.

(34) Bavykin, D. V.; Gordeev, S. N.; Moskalenko; Lapkin A. A.; Walsh, F. C. *J. Phys. Chem. B* **2005**, *109*, 8565.